

A kernel-independent sum-of-Gaussians method by de la Vallée-Poussin sums

Jiuyang Liang¹, Zixuan Gao², and Zhenli Xu^{*1,3}

¹School of Mathematical Sciences, Shanghai Jiao Tong University, Shanghai, 200240, P. R. China

²Zhiyuan College, Shanghai Jiao Tong University, Shanghai 200240, China

³Institute of Natural Sciences and MOE-LSC, Shanghai Jiao Tong University, Shanghai, 200240, P. R. China

Abstract

Approximation of interacting kernels by sum of Gaussians (SOG) is frequently required in many applications of scientific and engineering computing in order to construct efficient algorithms for kernel summation and convolution problems. In this paper, we propose a kernel-independent SOG method by introducing the de la Vallée-Poussin sum and Chebyshev polynomials. The SOG works for general interacting kernels and the lower bound of bandwidths of resulted Gaussians is allowed to be tunable so that the Gaussians can be easily summed by fast Gaussian algorithms. The number of terms can be further reduced via the model reduction based on square root factorization. Numerical results on the accuracy and model reduction efficiency show attractive performance of the proposed method.

Key words. Sum-of-Gaussians approximation, interaction kernels, de la Vallée-Poussin sum, model reduction

AMS subject classifications. 65D15, 42A16, 70F10

1 Introduction

For a given smooth function $f(x)$ for $x \in D$ with D a finite interval and an error tolerance ε , we consider the approximation of this function by the sum of Gaussians (SOG),

$$\max_{x \in D} \left| f(x) - \sum_j w_j e^{-t_j x^2} \right| < \varepsilon \max_{x \in D} |f(x)|, \quad (1.1)$$

where w_j and $1/\sqrt{t_j}$ represent the weight and the bandwidth of the j th Gaussian, respectively. Over the past decades, the SOG approximation has attracted wide interest since it can be useful in many applications of scientific computing such the approximation of the convolution kernel in physical space [1, 2, 3], the acceleration of the kernel summation problem

*xuzl@sjtu.edu.cn

[4, 5] and efficient nonreflecting boundary conditions for the wave and the Schrödinger equations [6, 7, 8, 9]. Generally, radial basis functions and potential field functions have kernels of the form $f(x) = f(\|\mathbf{x}\|)$ for $\mathbf{x} \in \mathbb{R}^d$, such as the power kernel $\|\mathbf{x}\|^{-s}$ with $s > 0$, the Hardy multiquadric $\sqrt{\|\mathbf{x}\|^2 + s^2}$, the Matérn kernel [10] and the thin-plate spline $\|\mathbf{x}\|^2 \log \|\mathbf{x}\|$. An SOG approximation to these kernels is particularly useful as a Gaussian function can simply achieve the separation of variables such that the convolution of $f(x)$ can be computed as the summation of products of d one-dimensional integrals, dramatically reducing the cost.

The solution of (1.1) is an extensively studied subject in literature [11, 12, 13, 14, 15, 16, 17, 18, 19, 20, 21]. One way to construct the SOG expansion is via the best rational approximation or the sum-of-exponentials (SOE) approximation, which is based on the fact that the Laplace transform of a SOE approximation of function $f(x)$ is a rational approximation of the Laplace transform of the function. When the kernel is radially symmetric, the SOG approximation is equivalent to the SOE approximation by a simple change of variable $y = \sqrt{x}$. If one does not restrict the bound of the Gaussian bandwidths, the integral representation of the kernel can be a significant tool. For example, the power function x^{-s} has the following inverse Laplace transform expression [12],

$$x^{-s} = \frac{1}{\Gamma(s)} \int_{-\infty}^{\infty} e^{-e^t x + st} dt, \quad (1.2)$$

with $\Gamma(\cdot)$ being the Gamma function. A suitable quadrature rule to Eq.(1.2) yields an explicit discretization to obtain a sum of exponentials. Constructing the SOG approximation from integral representation is superficially attractive due to the controllable high accuracy with the number of Gaussians. The integral form for general kernels by the inverse Laplace transform can be found in Dietrich and Hackbusch [14].

Another important approach for the SOG is the least squares approximation. A straightforward use of the least squares method will be less accurate due to the difficulty of solving the ill-conditioned matrix. The least squares problem can be solved by employing the divided-difference factorization and the modified Gram-Schmidt method to significantly improve the accuracy [21]. Greengard *et al.* [3] developed a black-box approach for the SOG of radially symmetric kernels. This approach allocates a set of logarithmically equally spaced points t_j lying on the positive real axis, then a set of sampling points x_i is constructed via adaptive bisections. Then the fitting matrix A with entry $A_{ij} = e^{-t_j x_i}$ and the right hand vector b with $b_i = f(x_i)$ are constructed. After one obtains the weights by solving the least squares problem, the square root method in model reduction [22] is introduced to reduce the number of exponentials and achieve a near-optimal SOE approximation.

Function approximation using Gaussians is a highly nonlinear problem and the design of such approximations for t_j such that it is bounded by a positive number (i.e., the lowerbound of bandwidths is independent of the number of Gaussians) is nontrivial. In applications with fast Gauss transform (FGT) [23, 24] to calculate the kernel summation problem with kernel approximated by the SOG, a small lowerbound of bandwidths will seriously reduce the performance of the algorithm. Due to this issue, it was reported [25] that the FGT is less useful for summing Gaussian radial basis function series, in spite of that Gaussian radial basis function interpolation has been widely employed in many applications such as machine learning problems. In this work, we propose a novel kernel-independent SOG method which

preserves both high precision and a tunable lowerbound of bandwidths. We construct the Gaussian approximation of the kernel by the de la Vallée-Poussin (VP) sum [26, 27] via a variable substitution. The variable substitution introduces a parameter n_c which allows to tune the minimal bandwidth of the Gaussians. Additionally, the model reduction can be further used to reduce the number of Gaussians, reaching an optimized SOG approximation.

The remainder of the paper is organized as follows. In Section 2, we derive the kernel-independent SOG approach and discuss the technique details. In Section 3, we perform numerical examples to demonstrate the performance of the new SOG scheme for different kernels. Concluding remarks are given in Section 4.

2 Sum-of-Gaussians approximation

In this section, we consider the problem of approximating functions on a finite real interval by linear combination of Gaussians, i.e., we approximate kernel function $f(x)$ by sum of p Gaussians,

$$f_p(x) = \sum_{j=1}^p w_j e^{-x^2/s_j^2}, \quad (2.1)$$

where w_j and s_j are weights and bandwidths, respectively. We define $s_p = \min_j |s_j|$ as the minimal bandwidth of the Gaussians.

2.1 de la Vallée-Poussin sums

We introduce the VP sum to obtain an SOG expansion. Let $f(x)$ be a smooth function defined on the positive axis, $x \geq 0$. We assume $f(x)$ has a limit at infinity. Without loss of generality, we assume the limit is zero, $\lim_{x \rightarrow \infty} f(x) = 0$. We introduce the variable substitution

$$x = \sqrt{-n_c \log \left(\frac{1 + \cos t}{2} \right)}, \quad t = [0, \pi], \quad (2.2)$$

where $t \leftrightarrow x$ is a one-to-one mapping. Parameter n_c is a positive constant, which determines the specified lowerbound of bandwidths. Let $\varphi(t) = f(x)$, which is smooth on $[0, \pi]$. We have $\varphi(0) = f(0)$ and $\varphi(\pi) = f(\infty) = 0$. We make an even prolongation of $\varphi(t)$ on $[-\pi, \pi]$ such that $\varphi(t)$ can be treated as an even periodic function with 2π period in $(-\infty, \infty)$.

The VP sum of $\varphi(t)$ is defined by (see [28] for reference),

$$V_n[\varphi(t)] = \frac{1}{n} \sum_{\ell=n}^{2n-1} S_\ell[\varphi(t)], \quad (2.3)$$

where

$$S_\ell[\varphi(t)] = \sum_{k=0}^{\ell} a_k \cos(kt), \quad (2.4)$$

is the Fourier partial sum of $\varphi(t)$ and the Fourier coefficients a_k are defined by,

$$a_k = \begin{cases} \frac{1}{\pi} \int_0^\pi \varphi(t) dt, & \text{for } k = 0, \\ \frac{2}{\pi} \int_0^\pi \varphi(t) \cos(kt) dt, & \text{for } k \geq 1. \end{cases} \quad (2.5)$$

The VP sum (2.3) can be reorganized into two components,

$$V_n[\varphi(t)] = S_n[\varphi(t)] + \sum_{\ell=1}^{n-1} \left(1 - \frac{\ell}{n}\right) a_{n+\ell} \cos[(n+\ell)t]. \quad (2.6)$$

We substitute the inverse mapping $t = \arccos(2e^{-x^2/n_c} - 1)$ to Eq. (2.6) and find,

$$f_p(x) = \sum_{\ell=0}^n a_\ell T_\ell(2e^{-x^2/n_c} - 1) + \sum_{\ell=1}^{n-1} \left(1 - \frac{\ell}{n}\right) a_{n+\ell} T_{n+\ell}(2e^{-x^2/n_c} - 1) \quad (2.7)$$

where $f_p(x) = V_n[\varphi(t)]$ is an approximation of $f(x)$, and by Theorem 1 it is an SOG with $p = 2n$. $T_m(x)$ is the Chebyshev polynomial of order m defined by,

$$T_m(x) = \cos(m \arccos(x)) = \sum_{\ell=0}^{\lfloor m/2 \rfloor} (-1)^\ell \binom{m-\ell}{2\ell} x^{m-2\ell} (1-x^2)^\ell. \quad (2.8)$$

By substituting Eq. (2.8) into Eq. (2.7) and rearranging the coefficients, we obtain the following Theorem 1.

Theorem 1. *Function $f_p(x)$ defined in Eq. (2.7) can be written as a sum of Gaussians,*

$$f_p(x) = \sum_{j=0}^{2n-1} w_j e^{-jx^2/n_c}, \quad (2.9)$$

where $p = 2n$ and coefficient w_j is given by,

$$w_j = \begin{cases} a_0 + \sum_{\ell=1}^n (-1)^\ell a_\ell + \sum_{\ell=1}^{n-1} (-1)^{n+\ell} \left(1 - \frac{\ell}{n}\right) a_{n+\ell}, & \text{for } j = 0, \\ 2^{2j} \sum_{\ell=j}^n (-1)^{\ell-j} \frac{\ell}{\ell+j} \binom{\ell+j}{\ell-j} a_\ell + \sum_{\ell=1}^{n-1} c_n^{j\ell} a_{n+\ell}, & \text{for } 1 \leq j \leq n, \\ \sum_{\ell=j-n}^{n-1} c_n^{j\ell} a_{n+\ell}, & \text{for } j > n, \end{cases} \quad (2.10)$$

and

$$c_n^{j\ell} = (-1)^{n+\ell-j} \left(1 - \frac{\ell}{n}\right) \frac{(n+\ell)}{n+\ell+j} \binom{n+\ell+j}{n+\ell-j} 2^{2j}.$$

Eq. (2.9) gives the expression of the SOG approximation with the bandwidth of j th Gaussian being $s_j = \sqrt{n_c/j}$ for $j > 0$. Note that the only approximation introduced in the SOG method is the numerical calculation of the Fourier coefficients Eq. (2.5), and the fast cosine transform can be employed for rapid evaluation of these coefficients.

Remark 1. *The minimal bandwidth in the Gaussians is $s_p = \sqrt{n_c/(2n-1)}$, thus n_c determines the bandwidth lowerbound of the SOG approximation. It asymptotically becomes constant if one sets $n_c \propto n$.*

2.2 Error estimate

We discuss the error estimate of the VP sum $V_n[\varphi(t)]$ to approximate $\varphi(t)$. We assume that $\varphi(t)$ is twice continuously differentiable in $[-\pi, \pi]$ except at $t = 0$, and analyze the errors when the function is not differentiable and first-order differentiable at $t = 0$, respectively.

When $\varphi(t)$ is not differentiable at $t = 0$, it was shown that $V_n[\varphi(t)]$ still converges to $\varphi(t)$ uniformly on \mathbb{R} , but the rate of convergence at $t = 0$ is much slower than at any other point. In this case, the error estimate of the VP sum was given in Boyer and Goh [29], and it is not difficult to follow the estimate to obtain the following result,

$$V_n[\varphi(0)] - \varphi(0) = -\frac{\ln 2}{n\pi} \sqrt{n_c} f'(0) + O\left(n^{-\frac{3}{2}}\right). \quad (2.11)$$

We now consider the case of $\varphi(t)$ being first-order differentiable at $t = 0$, and there is $f'(0) = 0$ since $f(x)$ is even. Many radial basis functions satisfy the condition $f'(0) = 0$ such as the inverse multiquadric kernel and the Matérn kernel with $\nu \geq 1$. In this case, the leading term in (2.11) vanishes, and the error order is higher. Actually, Theorem 2 shows that the error is the second order of convergence with respect to $1/n$, instead of $O(n^{-3/2})$.

Theorem 2. *Suppose that $V_n[\varphi(t)]$ is the n th VP sum of $\varphi(t)$ which is twice-differentiable on $[0, \pi]$ with period 2π and defined through Eq. (2.2) by $f(x)$. If $f'(0) = 0$, then we have*

$$V_n[\varphi(0)] - \varphi(0) = O\left(n^{-2}\right), \text{ and,} \quad (2.12)$$

$$V_n[\varphi(t)] - \varphi(t) = o\left(n^{-2}\right), \text{ for } t \neq 0. \quad (2.13)$$

Proof. We have $S_n[\varphi(t)]$ and $V_n[\varphi(t)]$ denoting the n th Fourier partial sum and the VP sum of $\varphi(t)$, respectively. Introduce the Fejér partial sum

$$\sigma_n[\varphi(t)] = \frac{1}{n+1} \sum_{\ell=0}^n S_\ell[\varphi(t)]. \quad (2.14)$$

The error of the VP sum can be written as

$$V_n[\varphi(t)] - \varphi(t) = 2\sigma_{2n}[\varphi(t)] - \sigma_n[\varphi(t)] - \varphi(t). \quad (2.15)$$

By using the Fejér kernel representation [27], one has,

$$\sigma_n[\varphi(t)] - \varphi(t) = \frac{1}{n\pi} \int_{-\pi}^{\pi} [\varphi(t+\xi) - \varphi(t)] \frac{\sin^2 \frac{n\xi}{2}}{2 \sin^2 \frac{\xi}{2}} d\xi. \quad (2.16)$$

Substituting Eq.(2.16) into Eq.(2.15), one gets,

$$V_n[\varphi(t)] - \varphi(t) = \frac{1}{n\pi} \int_{-\pi}^{\pi} [\varphi(t+\xi) - \varphi(t)] \frac{\cos n\xi - \cos 2n\xi}{4 \sin^2 \frac{\xi}{2}} d\xi. \quad (2.17)$$

Consider the case of $t = 0$. Eq.(2.17) can be decomposed into two parts I_1 and I_2 with

$$I_1 = \frac{1}{n\pi} \int_0^{\pi} (\varphi(\xi) - \varphi(0)) \frac{\cos n\xi - \cos 2n\xi}{4 \sin^2 \frac{\xi}{2}} d\xi \quad (2.18)$$

and

$$I_2 = \frac{1}{n\pi} \int_{-\pi}^0 (\varphi(\xi) - \varphi(0)) \frac{\cos n\xi - \cos 2n\xi}{4 \sin^2 \frac{\xi}{2}} d\xi. \quad (2.19)$$

First, we focus on I_1 , then decompose I_1 as two parts I_{11} and I_{12} , where

$$I_{11} = \frac{1}{n\pi} \int_0^{\pi} (\varphi(\xi) - \varphi(0)) (\cos n\xi - \cos 2n\xi) \left(\frac{1}{4 \sin^2 \frac{\xi}{2}} - \frac{1}{\xi^2} \right) d\xi \quad (2.20)$$

and

$$I_{12} = \frac{1}{n\pi} \int_0^\pi (\varphi(\xi) - \varphi(0))(\cos n\xi - \cos 2n\xi) \frac{1}{\xi^2} d\xi. \quad (2.21)$$

Since $1/4 \sin^2(\xi/2) - 1/\xi^2$ remains positive with an upper bound 0.15 and a lower bound 0.08 on $\xi \in [0, \pi]$. The each part of integrand of I_{11} is continuous on closed interval $[0, \pi]$. By the first mean value theorem for integrals to I_{11} , there exists a positive number M_1 such that

$$I_{11} = \frac{M_1}{n\pi} \int_0^\pi (\varphi(\xi) - \varphi(0))(\cos n\xi - \cos 2n\xi) d\xi. \quad (2.22)$$

By integration by parts, one gets

$$\begin{aligned} I_{11} &= \frac{M_1}{n\pi} \left[\left(\frac{1}{n} \sin n\xi - \frac{1}{2n} \sin 2n\xi \right) \frac{\varphi(\xi) - \varphi(0)}{\xi} \Big|_{\xi=0}^\pi - \right. \\ &\quad \left. \int_0^\pi \frac{d \frac{\varphi(\xi) - \varphi(0)}{\xi}}{d\xi} \left(\frac{1}{n} \sin n\xi - \frac{1}{2n} \sin 2n\xi \right) d\xi \right] \\ &= \frac{M_1}{n^2\pi} \int_0^\pi \frac{d \frac{\varphi(\xi) - \varphi(0)}{\xi}}{d\xi} \left(\sin n\xi - \frac{1}{2} \sin 2n\xi \right) d\xi \\ &= O\left(\frac{1}{n^2}\right), \end{aligned} \quad (2.23)$$

where the last two steps employ the conditions that $\varphi'(0) = 0$ and $\varphi''(0)$ exists.

For I_{12} , one can decompose I_{12} into two parts I_{121} and I_{122} , where

$$I_{121} = \frac{1}{n\pi} \int_0^{\frac{1}{n}} (\varphi(\xi) - \varphi(0))(\cos n\xi - \cos 2n\xi) \frac{1}{\xi^2} d\xi, \quad (2.24)$$

and

$$I_{122} = \frac{1}{n\pi} \int_{\frac{1}{n}}^\pi (\varphi(\xi) - \varphi(0))(\cos n\xi - \cos 2n\xi) \frac{1}{\xi^2} d\xi. \quad (2.25)$$

Note that $\cos n\xi - \cos 2n\xi$ is a monotonically increasing function which is non-negative on $[0, 1/n]$. Due to the existence of $f''(t)$, the rest part of the integrand of I_{121} is integrable and bounded. One employs the second mean value theorem for integrals to I_{121} , and finds that there exists a positive $M_2 \leq 1/n$ such that

$$I_{121} = \frac{1}{n\pi} (\cos 1 - \cos 2) \int_{M_2}^{\frac{1}{n}} \frac{\varphi(\xi) - \varphi(0)}{\xi^2} d\xi = O\left(\frac{1}{n^2}\right). \quad (2.26)$$

Note that $[\varphi(\xi) - \varphi(0)]/\xi^2$ is bounded on $[1/n, \pi]$. There exists a positive number M_3 such that

$$|I_{122}| \leq \frac{M_3}{n\pi} \left| \int_{\frac{1}{n}}^\pi (\cos n\xi - \cos 2n\xi) d\xi \right| = \frac{M_3(2 \sin 1 - \sin 2)}{2n^2\pi} = O\left(\frac{1}{n^2}\right). \quad (2.27)$$

Finally, combining these estimates, one gets,

$$I_1 = I_{11} + I_{12} = I_{11} + I_{121} + I_{122} = O\left(\frac{1}{n^2}\right). \quad (2.28)$$

Similarly, it holds,

$$I_2 = O\left(\frac{1}{n^2}\right). \quad (2.29)$$

Substituting these estimates for I_1 and I_2 into Eq. (2.17) completes the proof of the first equality in Eq. (2.12). For the case $t \neq 0$, the proof is similar and we omit the details. \square

Remark 2. When $\lim_{x \rightarrow \infty} f(x)$ doesn't exist, the above approach of constructing the SOG expansion has low accuracy because of the noncontinuity of the transformed function $\varphi(t)$. In order to achieve higher accuracy, one could truncate $f(x)$ at a required point, then connect a fast decreasing function behind the cutoff point such that a new function $f^*(x)$ to localize the kernel function. The higher-order differentiable properties of $f^*(x)$ can be kept.

2.3 Model reduction method for reduced number of Gaussians

In this section, we consider to reduce the number of Gaussians in the SOG expansion. We apply the square root method in model reduction [22, 30] for the purpose, which achieves a near optimal SOE approximation. That is, we find a q -term Gaussians for Eq.(2.9) that

$$\sum_{j=0}^{2n-1} w_j e^{-jx^2/n_c} \approx \sum_{\ell=1}^q \tilde{w}_\ell e^{-x^2/s_\ell^2}, \quad (2.30)$$

where $q < 2n - 1$ and the minimal bandwidth $s_q = \min_{\ell} |s_\ell| \approx \sqrt{n_c/(2n - 1)}$.

Suppose that $y = x^2$. The model reduction procedure first writes the left hand side of Eq. (2.30) (excluding $j = 0$) into the SOE expansion with parameter y , and then introduces the Laplace transform on it to obtain a sum-of-poles representation,

$$\mathcal{L} \left[\sum_{j=1}^{2n-1} w_j e^{-jy/n_c} \right] = \sum_{j=1}^{2n-1} \frac{w_j}{z + j/n_c}. \quad (2.31)$$

The sum-of-poles representation in Eq.(2.31) can be simply expressed as the following transfer function of a linear dynamical system

$$C(zI - A)^{-1}B = \sum_{j=1}^{2n-1} \frac{w_j}{z + j/n_c}, \quad (2.32)$$

where A is a diagonal matrix, B and C are column and row vectors, respectively and they reads,

$$\begin{aligned} A^{(2n-1) \times (2n-1)} &= -\text{diag} \left\{ \frac{1}{n_c}, \frac{2}{n_c}, \dots, \frac{(2n-1)}{n_c} \right\}, \\ B^{(2n-1) \times 1} &= \left(\sqrt{|w_1|}, \sqrt{|w_2|}, \dots, \sqrt{|w_{2n-1}|} \right)^T, \\ C^{1 \times (2n-1)} &= \left(\text{sign}(w_1) \cdot \sqrt{|w_1|}, \text{sign}(w_2) \cdot \sqrt{|w_2|}, \dots, \text{sign}(w_{2n-1}) \cdot \sqrt{|w_{2n-1}|} \right). \end{aligned} \quad (2.33)$$

The linear dynamical system with the coefficient matrices in Eq.(2.33) can be reduced using the balanced truncation [30] where the square root method can be used for the purpose. This procedure leads to a reduced system with coefficients $\tilde{A}^{q \times q}$, $\tilde{B}^{q \times 1}$ and $\tilde{C}^{1 \times q}$, such that the corresponding transfer function $\tilde{C}(zI - \tilde{A})^{-1}\tilde{B}$ satisfies

$$\sup_{z=i\mathbb{R}} \left| \tilde{C}(zI - \tilde{A})^{-1}\tilde{B} - C(zI - A)^{-1}B \right| \leq \tilde{\varepsilon}, \quad (2.34)$$

for a given tolerance $\tilde{\varepsilon}$. By employing the eigendecomposition and the inverse Laplace transform, one accomplishes the model reduction procedure, resulting in an optimized SOG approximation with q Gaussians Eq. (2.30).

We remark that the model reduction technique was originally designed for sum-of-poles approximation and the optimality of the resulting SOE approximation in the L^∞ norm is guaranteed by well-known results in control theory [22, 31]. However, since all the nodes lie in the left half of the complex plane, we are allowed to apply it directly to the reduction of SOG approximation because of the aforementioned connection between these two types of approximations [3]. The implementation of model reduction can also be obtained by employing the balance of Moore or the orthogonal-diagonal approach [30, 32].

3 Numerical results

In this section, we present numerical results to illustrate the performance of the SOG approximation method developed in this paper. We perform numerical calculations on a Intel TM core of clock rate 2.50 GHz with 24 GB of memory. Due to the requirement of high-precision matrix manipulation, we employ the GNU Multiple Precision Arithmetic Library (GMP) [33], the Multiple Precision Floating-Point Reliable Library (MPFR) [34] and the Multiple Precision Toolbox (MP) [35] in order to implement the model reduction procedure.

In our calculations, four different kernels are used to measure the performance of the algorithm. These are the Gaussian kernel f_{gauss} which has a small bandwidth $h = 0.1$, the inverse multiquadric kernel f_{imq} , the Ewald splitting kernel f_{ewald} and the Matérn kernel f_{matern} , expressed as,

$$f_{\text{gauss}}(x) = e^{-x^2/h^2}, \quad (3.1)$$

$$f_{\text{imq}}(x) = \frac{1}{\sqrt{1/2 + x^2}}, \quad (3.2)$$

$$f_{\text{ewald}}(x) = \frac{\text{erf}(\alpha x)}{x}, \quad (3.3)$$

$$f_{\text{matern}}(x) = \frac{(\sqrt{2\nu}|x|)^\nu K_\nu(\sqrt{2\nu}|x|)}{2^{\nu-1}\Gamma(\nu)}, \quad (3.4)$$

where $\text{erf}(x) = (2/\sqrt{\pi}) \int_0^x \exp(-u^2) du$ is the error function, K_ν is the modified Bessel function of the second kind of order ν and Γ is the Gamma function. We take parameter $\alpha = 1$ and $\nu = 2$ in the calculations. We remark that the Gaussian and the inverse multiquadratic kernels are mostly used radial basis functions which have been used in a broad range of data science and engineering problems [36, 37]. The Ewald splitting kernel f_{ewald} is the long-range part of the well-known Ewald summation [38, 39, 40] for Coulomb interaction and the parameter α describes the inverse of cutoff radius. Lastly, the Matérn kernel is also a radial basis function and often used as a covariance function in modeling Gaussian process [10], where the parameter ν describes the smoothness of the kernel.

We begin with the performance of the SOG to approximate the exact kernels with the increase of n , the number in the VP sum. To assess the accuracy, we compute the maximal relative error ϵ_∞ of the resulted SOG approximation $f_p(x)$ with $p = 2n$ in the case of without

the model reduction, which is defined by,

$$\epsilon_\infty = \frac{\max \{|f_p(x_i) - f(x_i)|, i = 1, \dots, M\}}{\max \{|f(x_i)|, i = 1, \dots, M\}}, \quad (3.5)$$

where $\{x_i, i = 1, \dots, M\}$ are monitoring points randomly distributed from $[0, 1]$ and we take $M = 1000$.

The results are given in Figure 1. In panel (a), we show the maximal relative errors for the four kernels with the increase of p . The number of Gaussians is $p = 2n$ as there is a constant term in the VP approximation. The parameter n_c is set to $n_c = \lceil n/4 \rceil$, and thus the minimal bandwidth is fixed to be $s_p \approx \sqrt{1/8}$, asymptotically independent of n . We observe that high accuracy of ϵ_∞ is achieved for all four kernels and that the convergence rate is very promising. It is mentioned that the Gaussian kernel f_{gauss} has very small bandwidth $h = 0.1$, but the SOG with all $s_j \gg h$ has rapid convergence with p is bigger than 100. In panel (b), the maximal relative error is shown as a function of the minimal bandwidth, where the total number of Gaussians is fixed to be $p = 10000$ and the value n_c is varying to tune the minimal bandwidth s_p . For the small Gaussian and the Matérn kernel, the observed accuracy is significantly improved when the minimal bandwidth is reduced. Whereas, the SOG approximation for the other two kernels seems not sensitive to the varying of minimal bandwidth since they are smoother functions and the high-frequency components in Fourier space are very small.

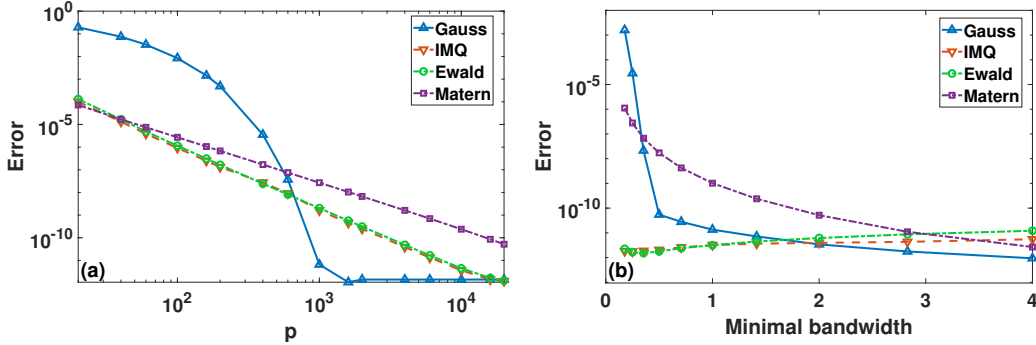


Figure 1: Dependence of the maximal relative error ϵ_∞ of the SOG approximation as: (a) function of p with fixed minimal bandwidth; and (b) function of the minimal bandwidth with fixed number of Gaussians. Data is shown for four kernels: the small Gaussian (Gauss), the inverse multiquadric (IMQ), the Ewald splitting (Ewald) and the Matérn kernel (Matern).

In practical calculations, the magnitude of the coefficients of Gaussians has close relation to the round-off error. It is necessary to check the effect of varying minimal bandwidth on the coefficient magnitudes. Figure 2 shows the maximal absolute value of the coefficients (maximum weight), $w_{\max} = \max\{|w_j|, j = 0, 1, \dots, p-1\}$, of the SOG expansion as function of minimal bandwidth s_p . The two panels shows results of fixed numbers of Gaussians, $p = 20$ and 40 , respectively. The relation between w_{\max} and the minimal bandwidth is substantially different for these kernels. Generally, as can be observed in Figure 2 (ab), the maximal coefficient magnitude increases with the number of Gaussians used for the SOG approximation. Within the calculated range of s_p , the maximum weight varies in about 3

number of digits for both $p = 20$ and 40 cases.

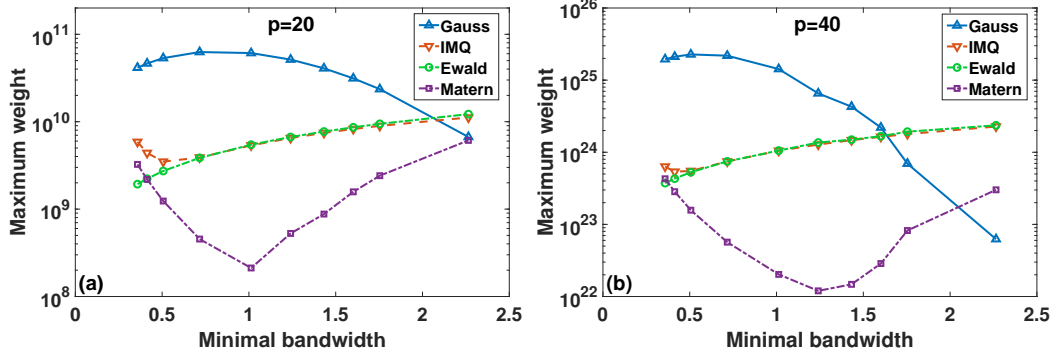


Figure 2: The maximal weight of the SOG approximation w_{\max} as a function of minimal bandwidth with two numbers of Gaussians: (a) $p = 20$ and (b) $p = 40$. Data for four kernels are calculated: small Gaussian, inverse multiquadratic, Ewald splitting and Matérn.

We next compare the SOG approximation constructed by the VP sum with that by the least squares method (LSM). For the LSM, we employ the complete orthogonal decomposition to compute the low-rank approximation of the fitting matrix such that the ill-conditioned matrix can be well resolved. In Figure 3(a-d), we show the comparison results for the four different kernels, where the relative errors as function of x and $x \in [0, 1]$ are displayed. Both the VP sum and the LSM are shown with two numbers of Gaussians, $p = 200$ and 800. Clearly, the VP-based SOG approximations provide more accurate results for all the four different kernels, thanks to the analytical manner of the VP sum.

Finally, we investigate the efficiency of the model reduction method used for the SOG approximation based on the VP sum. In Tables 1 and 2, we present the results with the model reduction of the SOG approximation for the inverse multiquadratic kernel and Matérn kernel where 100 initial Gaussians (with $n = 50$ for the VP sum) are used. The data of maximum weight \tilde{w}_{\max} , the minimal bandwidth s_q , and the maximum relative error ϵ_{∞} are shown for difference reduced numbers of Gaussians q . More than 30% of Gaussians for inverse multiquadratic and 50% of Gaussians for Matérn could be reduced under the same level of ϵ_{∞} as the original SOG. Interestingly, the maximum weight \tilde{w}_{\max} dramatically becomes small number with the use of the model reduction. With the decrease of Gaussians, \tilde{w}_{\max} will become smaller, and the minimum bandwidth s_q increases for the inverse multiquadratic kernel and slightly decreases for the Matérn kernel. These results demonstrate the model reduction method is efficient to obtain the optimized SOG approximation.

4 Conclusions

We have developed a high-accurate and kernel-independent SOG method for which the minimal bandwidth of Gaussians is controllable. This method is constructed by using the variable substitution and VP sums. The number of Gaussians is further reduced by employing the model reduction via square root approach. Such approximations can be combined with the Hermite expansion [41, 42] and the fast algorithms of [23, 43] to achieve efficient,

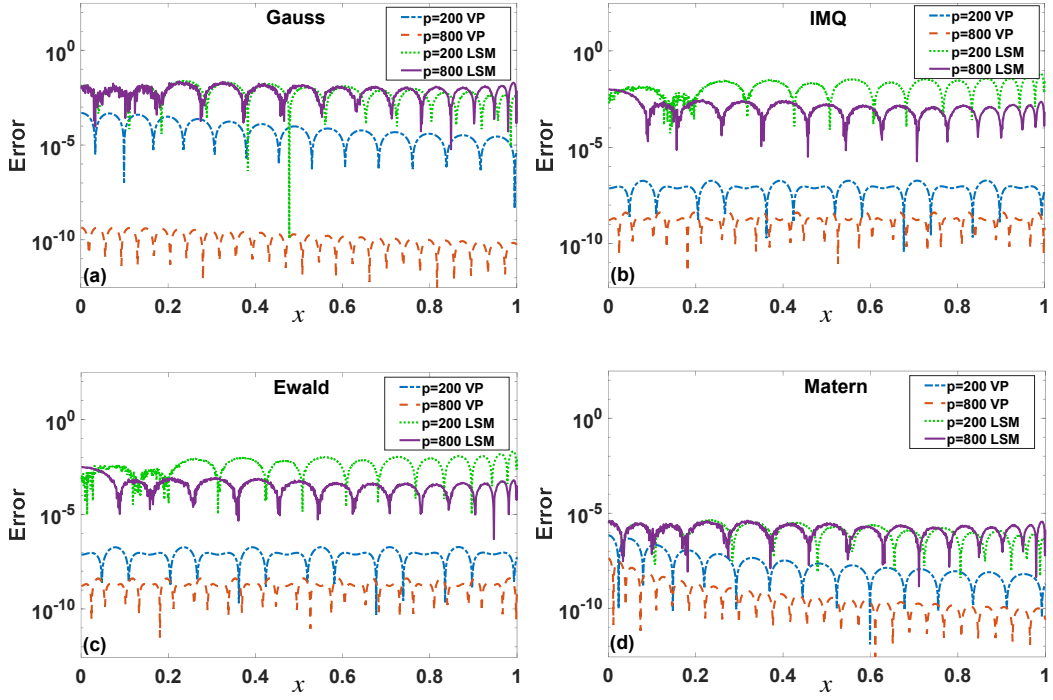


Figure 3: Relative error as function of x for the SOG approximations via VP-sums and LSM for four different kernels: (a) Gaussian; (b) inverse multiquadric; (c) Ewald splitting; and (d) Matérn. Results of the SOG methods with 200 and 800 Gaussians are shown.

Table 1: Model reduction with 100 initial Gaussians for f_{imq}

Reduced number q	\tilde{w}_{\max}	s_q	ϵ_{∞}
100	5.96e+68	0.361	2.36e-6
90	37.5	0.201	2.36e-6
70	13.7	0.346	2.66e-6
50	6.90	0.363	2.34e-5
30	2.31	0.421	1.87e-4
10	2.31	0.665	1.03e-2

Table 2: Model reduction with 100 initial Gaussians for f_{matern}

Reduced number q	\tilde{w}_{\max}	s_q	ϵ_{∞}
100	5.70e+64	0.361	3.87e-6
90	0.335	0.131	3.87e-6
70	0.467	0.122	3.88e-6
50	0.309	0.113	3.89e-6
30	0.246	0.116	5.68e-6
10	0.274	0.153	1.84e-5

accurate and robust methods for the fast evaluation of kernel summation and convolution problems, which will be studied in our future work.

Acknowledgement

The authors acknowledge the financial support from the Natural Science Foundation of China (Grant No. 21773165), the Strategic Priority Research Program of CAS (Grant No. XDA25010403) and the support from the HPC Center of Shanghai Jiao Tong University. The authors thank Prof. Shidong Jiang for some helpful comments.

References

- [1] G. Beylkin, C. Kurcz, L. Monzón, Fast convolution with the free space Helmholtz Green's function, *Journal of Computational Physics* 228 (8) (2009) 2770–2791.
- [2] A. Cerioni, L. Genovese, A. Mirone, V. A. Sole, Efficient and accurate solver of the three-dimensional screened and unscreened Poisson's equation with generic boundary conditions, *The Journal of Chemical Physics* 137 (13) (2012) 134108.
- [3] L. Greengard, S. Jiang, Y. Zhang, The anisotropic truncated kernel method for convolution with free-space Green's functions, *SIAM Journal on Scientific Computing* 40 (6) (2018) A3733–A3754.
- [4] H. Cheng, L. Greengard, V. Rokhlin, A fast adaptive multipole algorithm in three dimensions, *Journal of Computational Physics* 155 (2) (1999) 468–498.
- [5] N. Yarvin, V. Rokhlin, An improved fast multipole algorithm for potential fields on the line, *SIAM Journal on Numerical Analysis* 36 (2) (1999) 629–666.
- [6] B. Alpert, L. Greengard, T. Hagstrom, Rapid evaluation of nonreflecting boundary kernels for time-domain wave propagation, *SIAM Journal on Numerical Analysis* 37 (4) (2000) 1138–1164.
- [7] S. Jiang, L. Greengard, Fast evaluation of nonreflecting boundary conditions for the Schrödinger equation in one dimension, *Computers & Mathematics with Applications* 47 (6-7) (2004) 955–966.
- [8] S. Jiang, L. Greengard, Efficient representation of nonreflecting boundary conditions for the time-dependent Schrödinger equation in two dimensions, *Communications on Pure and Applied Mathematics* 61 (2) (2008) 261–288.
- [9] C. Lubich, A. Schädle, Fast convolution for nonreflecting boundary conditions, *SIAM Journal on Scientific Computing* 24 (1) (2002) 161–182.
- [10] J. Chen, L. Wang, M. Anitescu, A fast summation tree code for Matérn kernel, *SIAM Journal on Scientific Computing* 36 (1) (2014) A289–A309.
- [11] G. Beylkin, L. Monzón, On approximation of functions by exponential sums, *Applied and Computational Harmonic Analysis* 19 (1) (2005) 17 – 48.

- [12] G. Beylkin, L. Monzón, Approximation by exponential sums revisited, *Applied and Computational Harmonic Analysis* 28 (2) (2010) 131–149.
- [13] D. Braess, Asymptotics for the approximation of wave functions by exponential sums, *Journal of Approximation Theory* 83 (1) (1995) 93–103.
- [14] D. Braess, W. Hackbusch, On the efficient computation of high-dimensional integrals and the approximation by exponential sums, in: *Multiscale, nonlinear and adaptive approximation*, Springer, 2009, pp. 39–74.
- [15] D. Braess, W. Hackbusch, Approximation of $1/x$ by exponential sums in $[1, \infty)$, *IMA Journal of Numerical Analysis* 25 (4) (2005) 685–697.
- [16] J. W. Evans, W. B. Gragg, R. J. LeVeque, On least squares exponential sum approximation with positive coefficients, *Mathematics of Computation* 34 (149) (1980) 203–211.
- [17] A. F. Rodríguez, L. de Santiago Rodrigo, E. L. Guillén, J. M. R. Ascariz, J. M. M. Jiménez, L. Boquete, Coding Prony’s method in MATLAB and applying it to biomedical signal filtering, *BMC bioinformatics* 19 (1) (2018) 1–14.
- [18] A. A. Gonchar, E. A. Rakhmanov, Equilibrium distributions and degree of rational approximation of analytic functions, *Mathematics of the USSR-Sbornik* 62 (2) (1989) 305.
- [19] D. W. Kammler, Least squares approximation of completely monotonic functions by sums of exponentials, *SIAM Journal on Numerical Analysis* 16 (5) (1979) 801–818.
- [20] J. M. Varah, On fitting exponentials by nonlinear least squares, *SIAM Journal on Scientific and Statistical Computing* 6 (1) (1985) 30–44.
- [21] Exponential-sum fitting of radiative transmission functions, *Journal of Computational Physics* 24 (4) (1977) 416 – 444.
- [22] K. Glover, All optimal Hankel-norm approximations of linear multivariable systems and their L^∞ -error bounds, *International Journal of Control* 39 (6) (1984) 1115–1193.
- [23] L. Greengard, J. Strain, The fast Gauss transform, *SIAM Journal on Scientific and Statistical Computing* 12 (1) (1991) 79–94.
- [24] Rapid evaluation of radial basis functions, *Journal of Computational and Applied Mathematics* 180 (1) (2005) 51 – 70.
- [25] The uselessness of the Fast Gauss Transform for summing Gaussian radial basis function series, *Journal of Computational Physics* 229 (4) (2010) 1311 – 1326.
- [26] C. J. de La Vallée-Poussin, *Leçons sur l’approximation des fonctions d’une variable réelle*, Paris, 1919.
- [27] I. P. Natanson, *Constructive function theory*, Vol. 1, Ungar, 1964.
- [28] R. Albtoush, K. Al-Khaled, Approximation of periodic functions by Vallee Poussin sums, *Hokkaido Mathematical Journal* 30.

- [29] R. P. Boyer, W. M. Y. Goh, Generalized Gibbs phenomenon for Fourier partial sums and de la Vallée-Poussin sums, *Journal of Applied Mathematics and Computing* 37 (1-2) (2011) 421–442.
- [30] B. Moore, Principal component analysis in linear systems: controllability, observability, and model reduction, *IEEE Transactions on Automatic Control* 26 (1) (1981) 17–32.
- [31] K. Xu, S. Jiang, A bootstrap method for sum-of-poles approximations, *Journal of Scientific Computing* 55 (1) (2013) 16–39.
- [32] S. Gugercin, A. C. Antoulas, C. Beattie, \mathcal{H}_2 model reduction for large-scale linear dynamical systems, *SIAM Journal on Matrix Analysis and Applications* 30 (2) (2008) 609–638.
- [33] T. Granlund, “GNU MP: The GNU multiple precision arithmetic library”, version 6.1.2, <http://gmplib.org/>.
- [34] L. Fousse, G. Hanrot, V. Lefèvre, P. Pélicier, P. Zimmermann, “MPFR: A multiple-precision binary floating-point library with correct rounding”, *ACM Transactions on Mathematical Software* 33 (2) (2007) article 13, 15 pages.
- [35] B. Barrowes, Multiple Precision Toolbox for MATLAB, MATLAB Central File Exchange.
- [36] X.-G. Hu, T.-S. Ho, H. Rabitz, The collocation method based on a generalized inverse multiquadric basis for bound-state problems, *Computer Physics Communications* 113 (2-3) (1998) 168–179.
- [37] B. Scholkopf, Kah-Kay Sung, C. J. C. Burges, F. Girosi, P. Niyogi, T. Poggio, V. Vapnik, Comparing support vector machines with Gaussian kernels to radial basis function classifiers, *IEEE Transactions on Signal Processing* 45 (11) (1997) 2758–2765.
- [38] T. Darden, D. York, L. Pedersen, Particle mesh Ewald: An $N \cdot \log(N)$ method for Ewald sums in large systems, *The Journal of Chemical Physics* 98 (12) (1993) 10089–10092.
- [39] P. P. Ewald, Die berechnung optischer und elektrostatischer gitterpotentiale, *Annalen Der Physik* 369 (3) (1921) 253–287.
- [40] S. Jin, L. Li, Z. Xu, Y. Zhao, A random batch Ewald method for particle systems with Coulomb interactions, *arXiv*: 2010.01559.
- [41] H. Dym, H. P. McKean, *Fourier series and integrals*, Academic Press, New York, 1972.
- [42] E. Hille, A class of reciprocal functions, *Annals of Mathematics* (1926) 427–464.
- [43] M. Spivak, S. K. Veerapaneni, L. Greengard, The fast generalized Gauss transform, *SIAM Journal on Scientific Computing* 32 (5) (2010) 3092–3107.